The pure rotational spectrum of TiF (X 4 r):3d transition metal fluorides revisited

P. M. Sheridan, S. K. McLamarrah, and L. M. Ziurys

Citation: The Journal of Chemical Physics **119**, 9496 (2003); doi: 10.1063/1.1615753
View online: http://dx.doi.org/10.1063/1.1615753
View Table of Contents: http://scitation.aip.org/content/aip/journal/jcp/119/18?ver=pdfcov
Published by the AIP Publishing

The pure rotational spectrum of TiF ($X^4\Phi_r$): 3d transition metal fluorides revisited

P. M. Sheridan, S. K. McLamarrah, and L. M. Ziurys[a)]
Department of Chemistry, Department of Astronomy, and Steward Observatory, University of Arizona, Tucson, Arizona 85721

(Received 29 April 2003; accepted 13 August 2003)

The pure rotational spectrum of TiF in its $X\,^4\Phi_r(v=0)$ ground state has been measured using millimeter/sub-millimeter wave direct absorption techniques in the range 140–530 GHz. In ten out of the twelve rotational transitions recorded, all four spin–orbit components were observed, confirming the $^4\Phi_r$ ground state assignment. Additional small splittings were resolved in several of the spin components in lower J transitions, which appear to arise from magnetic hyperfine interactions of the ^{19}F nucleus. In contrast, no evidence for Λ-doubling was seen in the data. The rotational transitions of TiF were analyzed using a case (a) Hamiltonian, resulting in the determination of rotational and fine structure constants, as well as hyperfine parameters for the fluorine nucleus. The data were readily fit in a case (a) basis, indicating strong first order spin–orbit coupling and minimal second-order effects, as also evidenced by the small value of λ, the spin–spin parameter. Moreover, only one higher order term, η, the spin–orbit/spin–spin interaction term, was needed in the analysis, again suggesting limited perturbations in the ground state. The relative values of the a, b, and c hyperfine constants indicate that the three unpaired electrons in this radical lie in orbitals primarily located on the titanium atom and support the molecular orbital picture of TiF with a $\sigma^1\delta^1\pi^1$ single electron configuration. The bond length of TiF (1.8342 Å) is significantly longer than that of TiO, suggesting that there are differences in the bonding between 3d transition metal fluorides and oxides. © *2003 American Institute of Physics.* [DOI: 10.1063/1.1615753]

I. INTRODUCTION

Titanium is encountered in a wide variety of research areas. For example, because of its low density and exceptional corrosion resistance, the metal and its alloys are used in the construction of aircraft and marine vehicle equipment.[1] Metal oxides containing titanium have shown high dielectric and ferroelectric properties and thus appear to be useful in the design of microelectronic devices.[2,3] Titanium compounds are also employed as Ziegler–Natta type catalysts; cyclopentadienyl titanium species, for example, are used to polymerize olefins such as styrene and ethylene,[4] while bis(phenoxyimine)-titanium based molecules are currently being investigated for their unique regioselectivity in polymerization insertion reactions.[5] From an astronomical aspect, gas-phase titanium bearing species such as TiO and TiH have been identified in the spectra of cool M-type stars,[6,7] while titanium carbide crystals have been found in meteorites[8] and perhaps even in circumstellar gas.[9]

Small titanium containing molecules are additionally of interest for gas phase spectroscopy. From their spectra, electronic and geometric properties of these species can be elucidated, leading to a better understanding of the macroscopic characteristics of larger Ti-bearing compounds. Titanium has a $4s^2 3d^2$ valence electron configuration, however, such that Ti-bearing molecules usually have an extensive manifold of closely spaced electronic states which can perturb each other. Furthermore, high values of electron orbital and spin angular momenta often occur in such species. Despite these complexities, several titanium radicals have been studied to date via near-infrared and optical spectroscopy. For example, the $b\,^1\Pi - X\,^3\Delta$ transition of TiS, the $^4\Gamma - X\,^4\Phi$ band of TiH, and the $^3\Delta - X\,^3\Phi$ system of TiF^+ have been investigated;[10–12] TiF ($G\,^4\Phi - X\,^4\Phi$) and TiCH ($^2\Pi - X\,^2\Sigma$) have been studied as well.[13,14] Millimeter-wave and PPMODR work have also been conducted, but thus far have been limited to TiO ($X\,^3\Delta$), TiN ($X\,^2\Sigma$), and TiCl ($X\,^4\Phi$).[15,16] Hyperfine structure was observed in TiN, giving some insight into the bonding in titanium compounds.

One titanium radical of interest is TiF, partly because high resolution data on the 3d transition metal fluorides, in general, are limited. While electronic spectra of these species have been recorded,[17–19] they are certainly not as well characterized as their oxide counterparts.[20] For example, pure rotational spectra exist only for ScF, CrF, FeF, NiF, and CuF;[21–25] in fact, only in the past year has the first high-resolution optical study of VF been conducted.[17] While these molecules are expected to exhibit highly ionic bonds, some, such as FeF,[23] show signs of covalent character.

TiF has been the subject of relatively few spectroscopic investigations. It was first observed in absorption using flash heating techniques by Diebner and Kay in 1969, who assigned the ground state as $^4\Sigma^-$.[26] Additional studies conducted by Chantalic, Deschamps, and Pannetier[27] again indicated a $^4\Sigma^-$ ground state. Shenyavskaya and Dubov in 1985 conducted further optical work, resulting in the reas-

a)Telephone: 1-520-621-6525; Fax: 1-520-621-1532; Electronic mail: lziurys@as.arizona.edu

signment of the electronic ground term as $^2\Delta$.[28] Very recently, Ram *et al.* have observed the spectrum of TiF in emission by Fourier transform techniques and by laser excitation spectroscopy, performing the first rotational analysis.[13] In their work, the ground state of TiF was once again reassigned, this time as $^4\Phi$. Their assignment was partly based on theoretical work by Harrison,[29] and in analogy to TiH ($X\,^4\Phi$).[11] Subsequent calculations by Boldyrev and Simons[30] for TiF again suggested a $^4\Phi$ ground state. Conclusive experimental evidence for this assignment, however, has not been obtained to date.

Here we present the first measurement of the pure rotational spectrum of the TiF radical using millimeter/sub-mm direct absorption methods. Multiple rotational transitions were recorded for the main titanium isotopomer, ^{48}TiF, each consisting of four fine structure components, which definitively establish the ground state of the molecule as $X\,^4\Phi_r$. In addition, magnetic hyperfine splittings, resulting from the ^{19}F nucleus, have been observed. These data have been modeled using a Hund's case (a) effective Hamiltonian, leading to the determination of rotational, fine structure, and hyperfine parameters. In this paper we present these results, interpret the constants and discuss their implications for bonding in $3d$ transition metal flourides.

II. EXPERIMENT

The pure rotational spectrum of TiF was measured using one of the quasi-optical millimeter/sub-millimeter wave direct absorption spectrometers of the Ziurys group. The major features of this instrument are outlined in Ziurys *et al.*,[31] except that offset ellipsoidal mirrors are used as the focusing elements in this case, resulting in a different optics path. Also, a pathlength modulator is employed to improve baseline stability. The reaction chamber has a robust doubled-walled construction, which enables the melting of transition metals in a Broida-type oven attached to the cell.

The synthesis of TiF was particularly difficult because of the high melting point and reactivity of titanium. Several modifications to the oven were necessary in order to successfully vaporize this metal: First of all, crucibles constructed of boron nitride had to be used instead of the usual alumina type; liquid titanium was found to react destructively with alumina. Second, the oven electrodes, normally made of steel or a steel alloy, had to be constructed out of molybdenum in order to withstand the oven temperatures. Also, zirconia felt had to be placed around the top of the crucible in order to prevent liquid titanium from boiling over and onto the heating element. To create TiF, titanium vapor was first produced by the oven from heating a solid metal rod. It was then reacted with 3–5 mTorr of SF_6, which was introduced into the reaction chamber from underneath the oven. Neither a carrier gas nor a dc discharge was necessary for molecular synthesis. Although titanium has several isotopes, only data for the main isotope, ^{48}Ti, were recorded.

Final measurements of the rotational transitions were made from an average of one scan in increasing frequency, and the other in decreasing frequency, covering the same 5 MHz range. For the lowest frequency measurements, an average of two such scan pairs was found necessary to achieve adequate signal-to-noise ratios. In order to obtain the center frequency of each transition, Gaussian curves were fit to the line profiles. Typical linewidths ranged from 360 kHz at 142 GHz to 1230 kHz at 523 GHz.

III. RESULTS

The ground state of TiF was initially assumed to be $^4\Phi_r$ for the purpose of our initial spectroscopic search. In this state, spin–orbit coupling results in four fine structure levels per rotational transition, labeled by quantum number Ω. Furthermore, these levels may be split again due to Λ-doubling. Although this interaction is thought to be negligible for molecules with high orbital angular momentum, lambda-doubling has been observed in pure rotational spectra of CoH ($X\,^3\Phi_i$) and in the ground state of CoF, as deduced from studies of the $^3\Phi - X\,^3\Phi$ transition.[32,33] Also, magnetic hyperfine coupling due to the ^{19}F nucleus ($I=1/2$) may be present, as observed in FeF in its $X\,^6\Delta_i$ state.[23]

Searches for the rotational spectrum of TiF were aided by the optical work of Ram *et al.*,[13] in which effective rotational constants of each fine structure component had been determined. Individual spin components were therefore readily located by scanning only a few hundred MHz, confirming the ground state assignment. Initially, the higher J transitions were studied. Here the two higher Ω ladders ($\Omega=7/2$ and 9/2) were found to consist of closely-spaced doublets; their separation varied from approximately 2 MHz in the $\Omega=7/2$ ladder to 3 MHz in the $\Omega=9/2$ component. Furthermore, this splitting decreased in magnitude with increasing J, ruling out lambda-doubling interactions as their origin. In addition, transitions in the $\Omega=5/2$ sub-level appeared somewhat broader than expected, although the $\Omega=3/2$ signals had typical line widths. The closely-spaced doublets were attributed to hyperfine interactions of the ^{19}F nucleus, which would be expected to decrease with increasing J.

The pure rotational data recorded for TiF are presented in Table I. As the table shows, twelve rotational transitions were measured in the frequency range 140–530 GHz. For ten of these transitions, all four fine structure components were observed with the relative intensities decreasing as the Ω value increased, definitively establishing the ground state of TiF as $^4\Phi_r$. The spin components also appeared to be regularly spaced as well, suggesting that spin–orbit coupling dominates the fine structure. In the higher J transitions, the fluorine hyperfine splittings were only observable in the $\Omega=9/2$ and 7/2 ladders, although the $\Omega=5/2$ lines were unusually broad. As J decreased, the splitting increased such that it was eventually resolved in the $\Omega=5/2$ ladder at the $J=18.5\leftarrow 17.5$ transition and in the $\Omega=3/2$ ladder at the $J=13.5\leftarrow 12.5$ transition.

Representative spectra of TiF are shown in Figs. 1 and 2. In Fig. 1, a spectrum of the $\Omega=3/2$ spin component of the $J=21.5\leftarrow 20.5$ transition near 469.7 GHz is presented. The spectrum consists of a single feature, as the hf structure is collapsed in this ladder at this high J value. In Fig. 2, the $\Omega=9/2$ spin–orbit component of the $J=20.5\leftarrow 19.5$ transition near 456.5 GHz is shown. Here the hf doublet is clearly visible, indicated by the respective F quantum numbers. In

TABLE I. Measured rotational transitions for TiF ($X\,^4\Phi_r$): (v=0).[a]

$J+1\leftarrow J$	$F+1\leftarrow F$	Ω	ν_{obs}	$\nu_{obs-calc}$	$J+1\leftarrow J$	$F+1\leftarrow F$	Ω	ν_{obs}	$\nu_{obs-calc}$
6.5←5.5	6← 5	1.5	142 130.638	−0.101		18←17	1.5	382 422.304	0.161
	7← 6	1.5	142 125.283	0.093		17←16	2.5	384 829.420	0.222
	6← 5	2.5	143 034.798	−0.101		18←17	2.5	384 827.632	−0.206
	7← 6	2.5	143 023.571	−0.039		17←16	4.5	389 852.043	−0.164
9.5←8.5	9← 8	1.5	207 703.507	−0.025		18←17	4.5	389 848.279	0.123
	10← 9	1.5	207 701.270	0.003	18.5←17.5	18←17	1.5	404 241.985	−0.077
	9← 8	2.5	209 019.847	0.007		19←18	1.5	404 241.985	0.114
	10← 9	2.5	209 014.655	−0.074		18←17	2.5	406 783.622	0.070
	9← 8	3.5	210 369.579	−0.082		19←18	2.5	406 782.206	−0.149
	10← 9	3.5	210 361.072	−0.082		18←17	3.5	409 388.332	0.035
	9← 8	4.5	211 769.550	0.073		19←18	3.5	409 385.767	−0.176
	10← 9	4.5	211 757.027	0.065		18←17	4.5	412 087.036	−0.070
10.5←9.5	10← 9	1.5	229 556.230	−0.012		19←18	4.5	412 083.552	0.127
	11←10	1.5	229 554.452	−0.041	20.5←19.5	20←19	1.5	447 864.621	0.099
	10← 9	2.5	231 009.810	0.004		21←20	1.5	447 864.621	0.157
	11←10	2.5	231 005.651	−0.015		20←19	2.5	450 673.700[b]	−0.381
	10← 9	3.5	232 500.158	−0.095		21←20	2.5	450 673.700[b]	0.559
	11←10	3.5	232 493.213	−0.058		20←19	3.5	453 553.392	0.183
	10← 9	4.5	234 045.720	−0.014		21←20	3.5	453 551.256	−0.005
	11←10	4.5	234 035.453	0.045		20←19	4.5	456 535.547	−0.088
12.5←11.5	12←11	1.5	273 252.290	0.074		21←20	4.5	456 532.474	−0.064
	13←12	1.5	273 251.054	−0.094	21.5←20.5	21←20	1.5	469 666.659	−0.075
	12←11	2.5	274 979.759	0.095		22←21	1.5	469 666.659	−0.070
	13←12	2.5	274 976.791	−0.017		21←20	2.5	472 609.283[b]	−0.321
	12←11	3.5	276 750.771	0.058		22←21	2.5	472 609.283[b]	0.517
	13←12	3.5	276 745.647	−0.101		21←20	3.5	475 625.367	0.221
	12←11	4.5	278 586.761	−0.043		22←21	3.5	475 623.369	0.009
	13←12	4.5	278 579.477	0.104		21←20	4.5	478 748.469	−0.036
13.5←12.5	13←12	1.5	295 094.922	0.080		22←21	4.5	478 745.702	0.061
	14←13	1.5	295 093.981	−0.025	22.5←21.5	22←21	1.5	491 462.521	−0.009
	13←12	2.5	296 958.889	0.054		23←22	1.5	491 462.521	−0.050
	14←13	2.5	296 956.403	−0.013		22←21	2.5	494 537.916[b]	−0.282
	13←12	3.5	298 869.789	0.024		23←22	2.5	494 537.916[b]	0.468
	14←13	3.5	298 865.325	−0.162		22←21	3.5	497 689.716	0.114
	13←12	4.5	300 850.750	0.060		23←22	3.5	497 687.828	−0.129
	14←13	4.5	300 844.138	−0.107		22←21	4.5	500 953.309	0.032
16.5←15.5	16←15	1.5	360 597.403	−0.171		23←22	4.5	500 950.642	0.026
	17←16	1.5	360 597.403	0.208	23.5←22.5	23←22	1.5	513 251.593	−0.014
	16←15	2.5	362 869.367	0.146		24←23	1.5	513 251.593	−0.095
	17←16	2.5	362 867.599	−0.068		23←22	2.5	516 459.256[b]	−0.281
	16←15	3.5	365 197.688	0.010		24←23	2.5	516 459.256[b]	0.391
	17←16	3.5	365 194.829	0.068		23←22	3.5	519 746.260	0.030
	16←15	4.5	367 610.742	0.014		24←23	3.5	519 744.630	−0.078
	17←16	4.5	367 606.330	0.093		23←22	4.5	523 149.537	−0.038
17.5←16.5	17←16	1.5	382 422.304	−0.116		24←23	4.5	523 147.015	−0.078

[a]In MHz.
[b]Blended lines, not included in the fit.

both figures there are a few unidentified features marked by asterisks.

The regularity of the spacing of the fine structure lines in TiF is illustrated in Fig. 3, which shows a stick figure of three widely separated transitions: $J=9.5\leftarrow 8.5$, $J=16.5\leftarrow 15.5$, and $J=23.5\leftarrow 22.5$. Approximate experimental intensities are displayed. Hyperfine structure is too small to be visible on this scale and thus is not shown. In all three spectra, the spin–orbit components are fairly evenly spaced, indicating that TiF closely follows a case (a) coupling scheme. The overall splitting of the fine structure components increases with J, as expected. The relative intensities of the spin components are consistent with the regular designation of the ground state.

IV. ANALYSIS

The pure rotational data for TiF were analyzed using a Hund's case (a) effective Hamiltonian of the form[23,34,35]

$$\hat{\mathbf{H}}_{\text{eff}}=\hat{\mathbf{H}}_{\text{rot}}+\hat{\mathbf{H}}_{\text{so}}+\hat{\mathbf{H}}_{\text{ss}}+\hat{\mathbf{H}}_{\text{so}}^{(3)}+\hat{\mathbf{H}}_{\text{hf}}. \tag{1}$$

The first three terms describe molecular rotation, first order spin–orbit coupling, and spin–spin coupling, respectively. The fourth expression in Eq. (1) contains the interaction characterized by the parameter η. This constant concerns the coupling of the spin–orbit and spin–spin interactions:[35]

$$\hat{\mathbf{H}}_{\text{so}}^{(3)}=\eta L_z S_z\left(S_z^2-\frac{3\mathbf{S}^2-1}{5}\right). \tag{2}$$

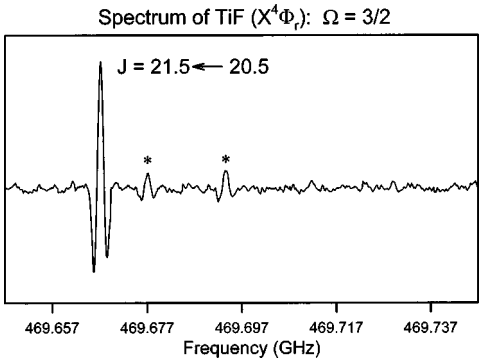

FIG. 1. Spectrum of the $J=21.5\leftarrow 20.5$ rotational transition of TiF ($X\ ^4\Phi_r$) in its lowest spin component, $\Omega=3/2$, observed near 469.7 GHz. The weaker lines marked by an asterisk are unidentified. Hyperfine splittings, which arise from interactions with the ^{19}F nuclear spin, are not apparent in these data and only appear at much lower J transitions. This spectrum is a single, 100 MHz scan obtained in approximately one minute.

The fifth term, $\hat{\mathbf{H}}_{\rm hf}$, includes the Frosch and Foley hyperfine constants a, b and c, which take into account both $\hat{\mathbf{I}}\cdot\hat{\mathbf{L}}$ and $\hat{\mathbf{I}}\cdot\hat{\mathbf{S}}$ interactions.

The TiF data were fit using this Hamiltonian in a least squares analysis in two stages. Initially, the centroids of each hyperfine doublet in all four spin–orbit components of the higher frequency transitions were analyzed to establish preliminary values of the rotational, spin–orbit, and spin–spin constants. In the process, it was found necessary to fix the spin–orbit constant, A, in order to achieve a satisfactory fit. (The value found by Ram *et al.*[13] for the spacing between the $\Omega=3/2$ and 5/2 components was used.) The inability to fit A is not surprising since TiF closely follows a case (a) coupling scheme. Once these constants were established, hyperfine interactions were then included in the analysis. Large residuals were obtained for rotational transitions higher than $J=19.5\leftarrow 18.5$ in the $\Omega=5/2$ spin–orbit component, because these lines had unresolved hyperfine splittings. In the final fit, these data were not included, as indicated in Table I.

The spectroscopic parameters determined for TiF are presented in Table II. The value of the rms of the millimeter-wave fit is 102 kHz, indicating the data were modeled adequately by the Hamiltonian in Eq. (1). In the process of the analysis, various higher order terms such as γ_s, the third order spin–rotation term,[36] and b_s, the third order Fermi contact hyperfine constant,[37] were included, but found not to improve the fit. Centrifugal distortion corrections to λ, η, and b were also not required. Hence, a limited number of spectroscopic parameters were needed for the final fit, in particular for the fine structure, where A, A_D, A_H, λ and η were only used.

Also presented in Table II are the constants derived from the optical study of TiF.[13] The two sets of constants are in fairly good agreement, although the values of A_D differ by

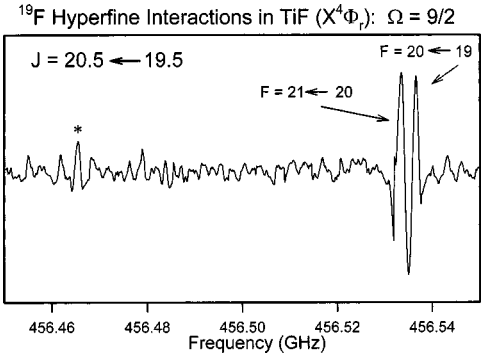

FIG. 2. Spectrum of the $J=20.5\leftarrow 19.5$ rotational transition of TiF ($X\ ^4\Phi_r$) in the $\Omega=9/2$ spin component recorded near 456 GHz. Here the ^{19}F hf interactions are clearly visible, splitting the transition into closely-spaced doublets, which are labeled by quantum number F. The weak feature marked by an asterisk is unidentified. This spectra is a single 100 MHz scan, lasting one minute in duration.

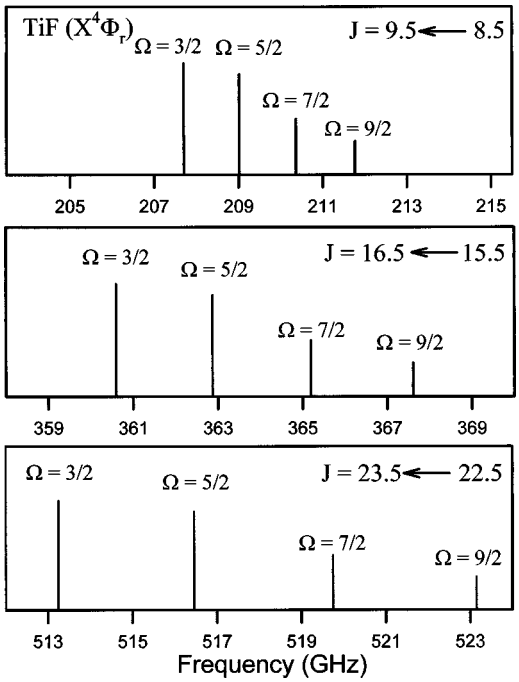

FIG. 3. A stick diagram illustrating the progression of the four spin components in TiF, over a wide range of frequency. The approximate relative intensities are shown, and each plot covers ~11 GHz. The separation of spin components increases with increasing J—almost a factor of two from the $J=9.5\leftarrow 8.5$ to the $J=23.5\leftarrow 22.5$ transitions. However, all four spin components are evenly spaced, even at high J, indicating strong spin–orbit coupling in TiF.

TABLE II. Spectroscopic parameters for TiF ($X\ ^4\Phi_r$): $v=0$.[a]

Parameter	Millimeter-wave	Optical[b]
B	11 040.0976(29)	11 037.5(2.4)
D	0.014 032 2(38)	0.0121(20)
A	1 018 000[c]	1 018 000
A_D	−3.456 63(84)	22.9
A_H	$3.22(10)\times 10^{-5}$	⋯
γ	⋯	10 400(1200)
λ	3681.2(7.0)	
η	−240.0(4.0)	
a	67.4(1.1)	
b	50(13)	
$b+c$	21.7(5.0)	
rms	0.102	

[a]In MHz; errors are 3σ and apply to the last quoted decimal places.
[b]From Ref. 13. Values originally quoted in cm^{-1}.
[c]Held fixed (see the text).

about an order of magnitude. This discrepancy is expected because the optical study utilized A_D and the spin–rotation constant, γ, whereas A_D, λ and η were used in the millimeter wave fit with no spin–rotation parameter. A_D and γ are usually highly correlated parameters;[39] thus the value of A_D will vary with that of γ.

V. DISCUSSION

A. A $^4\Phi$ ground state for TiF

The measurement of the millimeter-wave spectrum of TiF has confirmed the $^4\Phi_r$ ground electronic state, as suggested by Ram *et al.*[13] and Boldyrev and Simons.[30] No additional features beyond the four identified were observed in this study, supporting the quartet spin multiplicity. Additionally, the half-integer values of the rotational quantum number eliminate the possibility of a $^4\Sigma$ ground state, which is the next lowest lying term, according to theory.[30] (All attempts at fitting the data to a $^4\Sigma$ Hamiltonian were unsuccessful.) The lack of Λ-doubling interactions in the rotational spectrum also suggests a high value of Λ. The primary electron configuration for TiF is consequently (core) $8\sigma^2 3\pi^4 9\sigma^1 1\delta^1 4\pi^1$.

This study is only the second measurement of the pure rotational spectrum of a molecule in a $^4\Phi$ ground state (and the third in any Φ state). The first such species investigated, TiCl $(X\,^4\Phi_r)$, was also observed by millimeter-wave spectroscopy.[16] Interestingly, both these radicals were fit with relatively few (and identical) parameters, excluding hyperfine terms, despite the high values of angular momenta concerned. The only higher order constant needed in both cases was η, the spin–orbit/spin–spin interaction, which has a similar value for both TiCl (−332 MHz) and TiF (−240 MHz). The relatively simple analysis in both cases results from the presence of strong first order spin–orbit coupling and the lack of second-order spin–orbit effects. Second-order interactions, isoconfigurational or otherwise, result from the perturbations of nearby $^2\Phi$, $^2\Gamma$, $^2\Delta$, $^4\Gamma$, $^4\Phi$, and $^4\Delta$ excited states. According to Boldyrev and Simons,[30] the lowest lying excited state in both TiF (and TiCl) is $^4\Sigma^-$, which would not participate in these types of perturbations. The only other state in the energy manifold calculated for TiF is $^2\Delta$, which is predicted to be >2000 cm^{-1} above the ground $^4\Phi$ state,[30] and hence may be sufficiently far away in energy to have little effect.

Additional evidence for minimal second-order spin–orbit effects is the relatively small value of the spin–spin parameter in TiF ($\lambda=3681$ MHz). This constant has been shown to consist of two contributions: pure spin–spin interactions and second-order spin–orbit coupling, namely $\lambda=\lambda^{ss}+\lambda^{so}$. The second-order term is thought to dominate in heavier molecules.[38] Contributions to λ^{so} in TiF can occur via perturbations from doublet and quartet Γ, Φ, and Δ states, as mentioned. With the exception of the high lying $G\,^4\Phi$ state, there is little definitive spectroscopic data providing the energies of these other states, except for the theoretically-predicted $^2\Delta$ term.[30] Therefore, it is difficult to establish which terms actually contribute to λ^{so}.

The primary second-order spin–orbit perturber in TiCl is assumed to be the $C\,^4\Delta$ state, which lies 3300 cm^{-1} in energy above the $X\,^4\Phi$ state. (The A and B states are $^4\Sigma$ and $^4\Pi$.) It has the electron configuration $9\sigma^1 1\delta^1 10\sigma^1$. It is likely that a $^4\Delta$ state also exists in the manifold of TiF. The energy of the $^4\Delta$ state in titanium flouride in fact can be estimated from the spin–spin constant, under the assumption that $\lambda\approx\lambda^{so}$, using perturbation theory.[39] If the $^4\Delta$ state is the dominant perturber, then

$$\lambda^{so}=\frac{|\langle 4\pi|al_+|10\sigma\rangle|^2}{72(E_\Delta-E_\Phi)}, \tag{3}$$

where a is the one electron spin–orbit constant for the antibonding 4π orbital. An evaluation of the matrix element leads to $\langle 4\pi|al_+|10\sigma\rangle=\sqrt{6}\zeta(\mathrm{Ti})$, assuming that the 4π orbital is chiefly $3d_\pi$ in character and the 10σ orbital is primarily $3d_\sigma$, centered on the titanium atom (see Ref. 20). Alternatively, the Ti^+ spin–orbit constant may be a more appropriate choice, as suggested by recent calculations.[40] The value in Ti^+ is $\zeta=117$ cm^{-1}, which hardly varies from that of neutral titanium, which is 123 cm^{-1}. Using Eq. (3), $\zeta(Ti^+)$ and the λ value from Table II, the energy separation between the $X\,^4\Phi$ ground state and the $^4\Delta$ state in TiF is estimated to be $\Delta E\approx 9300$ cm^{-1}. This value is considerably larger than the $C\,^4\Delta-X\,^4\Phi$ separation in TiCl, which is 3300 cm^{-1}.[16] Because TiF is a lighter molecule, the $C\,^4\Delta-X\,^4\Phi$ separation will be larger than that in TiCl, but probably not by a factor of three. Other excited electronic states are perhaps contributing to λ^{so} to decrease its value. One such state is the isoconfigurational $^2\Phi$ level, for which

$$\lambda^{so}=\frac{3A^2}{16(E_{^2\Phi}-E_{^4\Phi})}. \tag{4}$$

Using the A value for the $X\,^4\Phi$ state, this equation suggests that the $^2\Phi$ state lies $\sim$1760 cm^{-1} higher in energy above the ground state. Hence, the $^2\Phi$ state is probably a major perturber as well.

Although lambda-doubling is thought to be negligible for Φ states, this interaction has in fact been observed in CoH $(^3\Phi_i)$ and CoF $(^3\Phi_i)$.[32,33] In CoH, lambda-doubling splittings on the order of >70 MHz were observed in LMR rotational spectra for the $\Omega=3$ spin–orbit component. This effect was unexpected, because the lambda-doubling matrix elements for $\Omega=3$ are diagonal only in $\tilde{q}_\Phi$, which is usually a small number.[32,41] (The $\tilde{o}_\Phi$ constant is largest in magnitude of the doubling parameters for triplet states.) The presence of significant lambda-doubling in the $\Omega=3$ ladder suggests the presence of a nearby $^3\Sigma$ state in CoH. The $\tilde{q}_\Phi$ parameter derived from the analysis of the CoH spectra is $\tilde{q}_\Phi=0.01667(24)$ MHz.[32] Because $\tilde{q}_\Phi$ scales approximately as B^6,[41] diatomic hydrides may be the extreme case.

The effects of Λ-doubling have also been reported for CoF, from Fourier transform spectroscopy of the $[10.3]^3\Phi_i-X\,^3\Phi_i$ transition.[19] Splittings attributable to this interaction were found in the $\Omega=2$ and 3 sub-bands for both electronic states. They were analyzed with a case (c) Hamiltonian, involving the effective Λ-doubling constant q. In the

TABLE III. Hyperfine parameters for TiF and related species.[a]

Molecule	a	b	c	b_F	$\psi^2(0)$[b]	$\Sigma_n\langle 1/r_n^3\rangle$[b]
TiF ($X\ ^4\Phi_r$)	67.4(1.1)	50(13)	−28(14)	41 (14)	0.0101	0.134
TiN ($X\ ^2\Sigma^+$)[c]		18.535(14)	0.166(21)	18.480(9)	0.057261	
FeF ($X\ ^6\Delta_i$)[d]	−0.45[e]	74.5(3.5)	51.7(3.5)	91.7(3.7)	0.0218	0.00090

[a]In MHz.
[b]In units of a_0^{-3}.
[c]Reference 42.
[d]Reference 23.
[e]Fixed value.

final fit, interestingly, only centrifugal distortion corrections to this parameter were used for the ground state, namely q_D and q_H.

In contrast to these cobalt radicals, there was no evidence of lambda-doubling in any spin component in TiF, at least up to $J=23.5$. In analogy to Δ states,[41] the sub-level that should exhibit the largest effect is the $\Omega=3/2$ ladder, where $\tilde{n}_\Phi$ would be the major contributing term. Unfortunately, the theory of Λ-doubling for Φ states has not been examined in any detail. However, using a Van Vleck transformation,[41] the $\tilde{n}_\Phi$ parameter can be approximated as

$$\tilde{n}_\Phi \propto \frac{B^3A^3}{(\Delta E)^5}, \tag{5}$$

where B and A are the rotational and spin–orbit constants, and $(\Delta E)^5$ are the energy differences between the $X\ ^4\Phi$ state and excited $^4\Delta$, $^4\Pi$, and $^4\Sigma$ states. The obviously small value of $\tilde{n}_\Phi$ must arise from significant energy differences between the ground and $^4\Pi$ and $^4\Delta$ states. (Theory predicts the $^4\Sigma$ state to be relatively close in energy.[30])

B. Interpretation of hyperfine parameters

In this study, the ^{19}F hyperfine splitting was modeled with a, b, and $(b+c)$ Frosh and Foley parameters. From these constants, the Fermi contact term b_F and spin dipolar constant c were calculated. These values are given in Table III. For comparison, hyperfine parameters for similar radicals are also listed; the sample is unfortunately limited to FeF[23] and TiN.[42] FeF and TiN have $X\ ^6\Delta$ and $X\ ^2\Sigma^+$ ground states, respectively.

The nuclear spin orbital constant, a, exhibits the greatest variations between these molecules. For example, a is ≈67 MHz for TiF but virtually zero for FeF. FeF has a $9\sigma^1 1\delta^3 4\pi^2 10\sigma^1$ electron configuration as opposed to $9\sigma^1 1\delta^1 4\pi^1$ for TiF, and thus has one additional electron in an orbital with angular momentum. (The σ orbitals do not contribute to a.) At first glance, one might expect the a parameter to be larger in FeF than TiF. However, the two π electrons in FeF have their spins aligned and therefore must have equal but opposite $\hat{\mathbf{I}}\cdot\hat{\mathbf{L}}$ matrix elements so as to not violate the Pauli principle: $\langle\lambda_i^+|a_iI_zl_{iz}|\lambda_i^+\rangle = -\langle\lambda_i^-|a_iI_zl_{iz}|\lambda_i^-\rangle$. Their $\hat{\mathbf{I}}\cdot\hat{\mathbf{L}}$ contributions therefore effectively cancel, in analogy to MnH.[43] The single electron in the π orbital in TiF, in contrast, can contribute fully to the nuclear spin–orbital interaction. (The single unpaired electron in the nonbonding δ orbital in both radicals is far enough away from the fluorine nucleus such that it has a negligible effect.)

The hf constant a is proportional to the inverse, cubed, of the distance r between the orbiting electrons and the nucleus possessing the spin I. Hence, this constant can be used to determine the expectation value of $\Sigma_n\langle 1/r_n^3\rangle$. For the fluorine atom, $\langle 1/r^3\rangle = 5.9\times10^{31}\ \mathrm{m}^{-3}$ or 8.77 in units of a_0^{-3},[44] which primarily represents the electron–nuclear separation for a $2p$ electron. The value for TiF is $9.07\times10^{29}\ \mathrm{m}^{-3}$ or $0.134a_0^{-3}$—over an order of magnitude smaller (see Table III), indicating that the unpaired electrons contributing to a in this radical are located, on average, much further from the F atom than a simple $2p$ orbital. The two contributing electrons are thought to reside in π and δ molecular orbitals, located primarily on the titanium atom. The small value derived for $\Sigma_n\langle 1/r_n^3\rangle$ supports this assumption.

Another comparison of interest are the respective Fermi contact terms. This parameter is directly proportional to the electron density at the nucleus with the spin, i.e., $b_F \propto[\psi^2(0)]$; thus, σ molecular orbitals are thought to make the principal contribution to this parameter. For TiF, $b_F \approx 41$ MHz, while the value for FeF is 91.7 MHz (see Table III). This factor of two increase occurs because FeF has two unpaired σ electrons, while TiF has one. TiN also has a single σ electron, but the smaller value for the nitride compound ($b_F = 18.5$ MHz) versus the fluoride in this case arises from the smaller magnetic moment of nitrogen relative to fluorine (0.404 versus 2.63 Bohr magnetons[44]). In fact, normalizing the Fermi contact terms by these moments, the $\psi^2(0)$ value in TiN is actually larger than in TiF (see Table III). This result can be attributed to the shorter bond length in TiN relative to TiF. Consequently, the single σ electron, located in the nonbonding 9σ orbital in both cases, can penetrate the nitrogen nucleus more effectively than that of fluorine.

Because of configuration interaction, elemental fluorine has an atomic Fermi contact term, $A_{\mathrm{iso}}(\mathrm{F}) = 52\,870$ MHz.[45] In contrast, b_F in TiF is substantially smaller. The percent of fluorine character retained on the formation of TiF is ≈0.08%. This result is not surprising; the σ electron in TiF is located in a nonbonding orbital primarily composed of the titanium 4s orbital, in analogy to TiN.[45] The electron density at the fluorine nucleus must be minimal.

The final parameter of interest is c, the dipolar constant, which is an anisotropic term. It is defined as[46]

$$c = \frac{3\mu_O\mu_I}{I}\sum_n \left\langle \frac{3\cos^2\theta_n - 1}{r_n^3} \right\rangle. \tag{6}$$

For TiF, the value of c is small and negative ($c = -28$ MHz), while the constant is positive and larger for

FeF ($c=51.7$ MHz), and virtually zero for TiN, as shown in Table III. Because TiN has only one unpaired σ electron, there is little to contribute to the anisotropy of the electron distribution around the nitrogen nucleus. Hence, the c parameter for TiN is very small. The differences in the magnitude of c for TiF and FeF can be interpreted in terms of their proposed electron configurations. For TiF the configuration is $9\sigma^1 1\delta^1 4\pi^1$; the 9σ orbital must be nonbonding and composed principally of the titanium $4s$ atomic orbital, in analogy with TiN.[45] The only contributors to c in TiF are the 1δ orbital ($3d_\delta$ orbital from the titanium atom) and the 4π antibonding orbital, composed principally of Ti $3d_\pi$ and F $2p_\pi$ atomic orbitals. In the case of FeF, where the principal configuration is $9\sigma^1 1\delta^3 4\pi^2 10\sigma^1$, there is an additional 4π electron as well as one in the 10σ antibonding orbital (a combination of the F $2p_\sigma$ and Ti $3d_\sigma$). These two electrons should increase the value of c relative to that in TiF. Indeed, c in FeF is a factor of two larger in absolute magnitude. Single electron configurations consequently can explain the relative hf parameters for TiF, FeF and TiN, and lend some credence to the molecular orbital picture of these species.

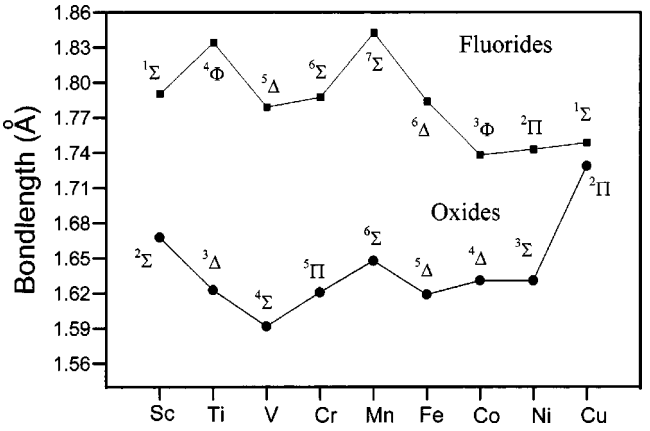

FIG. 4. A graph showing the periodic trends in bond lengths for the $3d$ transition metal oxides vs the fluorides. The oxides exhibit the characteristic ''double hump'' structure in this plot, i.e., the bond lengths increase from V to Mn and from Fe to Cu, indicating the competition between the addition of antibonding electrons vs core contraction. The fluorides show a similar trend, but with variations at titanium and copper. The increase in bond length at TiF likely results from the addition of an electron to the 4π antibonding orbital, which does not start to fill in the oxides until chromium.

C. Trends in 3*d* fluoride species

The bonding in alkali and alkaline-earth fluorides, in general, is thought to be largely ionic.[47] Transition metal fluorides might be expected to behave similarly. Theoretical calculations of TiF predict a $+0.82e$ charge on the titanium atom and a dipole moment of 3 Debye.[30] A large amount of ionic bonding character, however, may not apply to all of the $3d$ transition metals. As one moves to the right of titanium in the periodic table, the covalent character of the metal fluoride bond may be expected to increase, using simple electronegativity arguments. In fact, this increased covalency is predicted for FeF, where only 65% of the structure is predicted to be ionic.[23] A general comparison of the bonding in $3d$ transition metal fluorides would therefore be of great interest. Unfortunately, no comprehensive review on the transition metal fluorides exists, although $3d$ oxides and sulfides have been studied extensively.[20,48,49]

One metric by which $3d$ oxides (and sulfides) have been compared is via their experimentally-measured bond lengths as a function of the metal atom.[49] A so-called ''double hump'' structure is apparent in such a plot for the oxides, as shown in Fig. 4. There is an increase in bond length from V to Mn, and then another increase from Fe to Cu. This behavior is thought to occur because the 4π antibonding orbital does not start to fill until chromium and manganese. The M–O bond thus lengthens despite the orbital contraction that comes with increased nuclear charge.[49] This trend is repeated in the second half of the $3d$ row.

A plot of the bond lengths for the $3d$ fluorides, also presented in Fig. 4, does not quite show the same trends. The most notable difference occurs in the bond lengths, which are 0.2 Å larger in the fluorides relative to the corresponding oxides, with the exception of copper. This behavior suggests that the oxides have a more multiple bond character than the fluorides, which routinely shortens the bond distances. Other deviations from the oxide trend for the fluorides include the increase in bond length at titanium and the lack of an increase at copper. These trends diverge because the fluorides have an extra electron relative to the oxides; at the same time, with increasing atomic number, the $3d$ orbitals drop rapidly in energy relative to the $4s$, while the energies of the $2p$ orbitals (O or F) rise.[20] From ScO to TiO, the electron configuration changes from σ to $\sigma\delta$, i.e., the additional electron fills a nonbonding orbital; the increase in nuclear charge causes the orbitals to contract and the bond length decreases. From ScF to TiF, the configuration changes from σ^2 to $\sigma^1\delta^1\pi^1$, and the π antibonding orbital acquires an electron, which subsequently increases the bond length. The $\sigma^1\delta^1\pi^1$ configuration in TiF is generated because the $3d$ orbitals have dropped sufficiently in energy at titanium such that the 4π orbital is accessible. In addition, the $2p$ orbitals in fluorine are lower in energy relative to oxygen, which in turn decreases the 4π energy faster in the fluorides. In the oxides this orbital does not become occupied until CrO ($\sigma^1\delta^2\pi^1$); VO, unlike TiF, exhibits a $\sigma\delta^2$ configuration.

The difference in the trend at copper, on the other hand, is more problematic. Presumably the increase in bond distance for CuO results from the addition of another electron into the antibonding 4π orbital; core contraction apparently cannot overcome this effect. The creation of CuF also adds another electron to this antibonding orbital, but in this case the shell is completed to create a $^1\Sigma$ state. The filling of the 4π shell, perhaps coupled with stronger orbital contraction in the more electronegative fluorides, results only in a slight increase in bond distance.

VI. CONCLUSION

Studies of radicals in high spin states serve as tests of theory and angular momentum coupling. This investigation of TiF by pure rotational spectroscopy and subsequent spectral analysis has demonstrated that this $3d$ transition metal radical can readily be modeled with a simple case (a) Hamiltonian with very few higher order terms. The regularity of

the splittings of the spin–orbit components indicates that second-order effects are minimal. It is also notable that there is no evidence of lambda-doubling in the spectra, unlike other species in Φ states. An analysis of the ^{19}F hyperfine interactions results in parameters that are consistent with a $\sigma^1\delta^1\pi^1$ configuration, where the σ and δ orbitals have primarily nonbonding $3d$ metal character, and the π orbital is antibonding, formed from a linear combination of $3d_\pi$ and $2p_\pi$ atomic orbitals. Hence, to a first approximation, the molecular orbital picture can explain the bonding in TiF, which suggests some degree of covalent behavior. Titanium fluoride was found to have a bond length 0.2 Å longer than that in TiO, as is found for virtually all $3d$ fluorides relative to their oxide counterparts. The bond distance in TiF lengthens because of the addition of an electron to the 4π antibonding orbital, which does not begin to fill in the oxides until chromium. Although the $3d$ fluorides have similar periodic trends to the corresponding oxides, there are subtle differences which have yet to be fully investigated.

ACKNOWLEDGMENTS

This research was supported by National Science Foundation (NSF) Grant Nos. CHE-98-17707 and AST-02-04913. The authors would like to thank Dr. J. M. Brown for use of his Hamiltonian code. This work was also supported in part by a fellowship from Merck Research Laboratories.

[1] F. A. Cotton, G. Wilkinson, C. A. Murillo, and M. Bochmann, *Advanced Inorganic Chemistry*, 6th ed. (Wiley, New York, 1999).
[2] K. Woo, W. I. Lee, J. S. Lee, and S. O. Kang, Inorg. Chem. **42**, 2378 (2003).
[3] R. F. Cava, W. F. Peck, and J. J. Krajewski, Jr., Nature (London) **377**, 215 (1995).
[4] R. J. Maldanis, J. C. W. Chien, and M. D. Rausch, J. Organomet. Chem. **599**, 107 (2000).
[5] P. D. Hustad, J. Tian, and G. W. Coates, J. Am. Chem. Soc. **124**, 3614 (2002).
[6] R. E. S. Clegg, D. L. Lambert, and R. A. Bell, Astrophys. J. **234**, 188 (1979).
[7] R. Yerle, Astron. Astrophys. **73**, 346 (1979).
[8] T. J. Bernatowicz, S. Amari, E. K. Zinner, and R. S. Lewis, Astrophys. J. Lett. **373**, L73 (1991).
[9] G. Von Helden, A. G. G. M. Tielens, D. Van Heijnsbergen, M. A. Duncan, S. Hony, L. Waters, and G. Meijer, Science **288**, 313 (2000).
[10] A. S.-C. Cheung, Q. Ran, W. S. Tam, D. K.-W. Mok, and P. M. Yeung, J. Mol. Spectrosc. **203**, 96 (2000).
[11] O. Launila and B. Lindgren, J. Chem. Phys. **104**, 6418 (1996).
[12] C. Fosca, B. Pinchemel, D. Collet, and T. R. Huet, J. Mol. Spectrosc. **189**, 254 (1998).
[13] R. S. Ram, J. R. D. Peers, Y. Teng, A. G. Adam, A. Muntianu, P. F. Bernath, and S. P. Davis, J. Mol. Spectrosc. **184**, 186 (1997).
[14] M. Barnes, A. J. Merer, and G. F. Metha, J. Mol. Spectrosc. **181**, 168 (1997).
[15] K. Namiki, S. Saito, J. S. Robinson, and T. C. Steimle, J. Mol. Spectrosc. **191**, 176 (1998).
[16] A. Maeda, T. Hirao, P. F. Bernath, and T. Amano, J. Mol. Spectrosc. **210**, 250 (2001).
[17] R. S. Ram, P. F. Bernath, and S. P. Davis, J. Chem. Phys. **116**, 7035 (2002).
[18] B. Simard and O. Launila, J. Mol. Spectrosc. **168**, 567 (1994).
[19] A. G. Adam and W. D. Hamilton, J. Mol. Spectrosc. **206**, 139 (2001).
[20] A. J. Merer, Annu. Rev. Phys. Chem. **40**, 407 (1989).
[21] W. Lin, S. A. Beaton, C. J. Evans, and M. C. L. Gerry, J. Mol. Spectrosc. **199**, 275 (2000).
[22] T. Okabayashi and M. Tanimoto, J. Chem. Phys. **105**, 7421 (1996).
[23] M. D. Allen and L. M. Ziurys, J. Chem. Phys. **106**, 3494 (1997).
[24] M. Tanimoto, T. Sakamaki, and T. Okabayashi, J. Mol. Spectrosc. **207**, 66 (2001).
[25] T. Okabayashi, E. Yamazaki, T. Honda, and M. Tanimoto, J. Mol. Spectrosc. **209**, 66 (2001).
[26] R. L. Diebner and J. G. Kay, J. Chem. Phys. **51**, 3547 (1969).
[27] A. Chatalic, P. Deschamps, and G. Pannetier, C. R. Acad. Sci. **270**, 146 (1970).
[28] E. A. Shenyavskaya and V. M. Dubov, J. Mol. Spectrosc. **113**, 85 (1985).
[29] J. F. Harrison (unpublished).
[30] A. I. Boldyrev and J. Simons, J. Mol. Spectrosc. **188**, 138 (1998).
[31] L. M. Ziurys, W. L. Barclay, Jr., M. A. Anderson, D. A. Fletcher, and J. W. Lamb, Rev. Sci. Instrum. **65**, 1517 (1994).
[32] S. P. Beaton, K. M. Evenson, and J. M. Brown, J. Mol. Spectrosc. **164**, 395 (1994).
[33] R. S. Ram, P. F. Bernath, and S. P. Davis, J. Chem. Phys. **104**, 6949 (1996).
[34] J. M. Brown, M. Kaise, C. M. L. Kerr, and D. J. Milton, Mol. Phys. **36**, 553 (1978).
[35] J. M. Brown, D. J. Milton, J. K. G. Watson, R. N. Zare, D. L. Albritton, M. Horani, and J. Rostas, J. Mol. Spectrosc. **90**, 139 (1981).
[36] T. Nelis, J. M. Brown, and K. M. Evenson, J. Chem. Phys. **92**, 4067 (1990).
[37] A. S.-C. Cheung and A. J. Merer, Mol. Phys. **46**, 111 (1982).
[38] H. Lefebvre-Brion and R. W. Field, *Perturbations in the Spectra of Diatomic Molecules* (Academic, Orlando, 1986).
[39] J. M. Brown, E. A. Colbourn, J. K. G. Watson, and F. D. Wayne, J. Mol. Spectrosc. **74**, 294 (1979).
[40] C. Fosca, M. Bencheikh, and L. G. M. Pettersson, J. Phys. B **31**, 2857 (1998).
[41] J. M. Brown, A. S.-C. Cheung, and A. J. Merer, J. Mol. Spectrosc. **124**, 464 (1987).
[42] D. A. Fletcher, C. T. Scurlock, K. Y. Jung, and T. C. Steimle, J. Chem. Phys. **99**, 4288 (1993).
[43] T. D. Varberg, R. W. Field, and A. J. Merer, J. Chem. Phys. **95**, 1563 (1991).
[44] W. Weltner, Jr., *Magnetic Atoms and Molecules* (Dover, New York, 1983).
[45] C. W. Bauschlicher, Jr., Chem. Phys. Lett. **100**, 515 (1983).
[46] C. H. Townes and A. L. Schawlow, *Microwave Spectroscopy* (Dover, New York, 1975).
[47] L. B. Knight, Jr., W. C. Easley, W. Weltner, Jr., and M. Wilson, J. Chem. Phys. **54**, 322 (1971).
[48] I. Kretzschmar, D. Schröder, H. Schwarz, and P. B. Armentrout, in *Advances in Metal and Semiconductor Clusters* (Elsevier, New York, 2001), Vol. 5, p. 347.
[49] A. J. Bridgeman and J. Rothery, J. Chem. Soc. Dalton Trans. **2000**, 211.